Dynamics of magnetization of a uniaxial nanoparticle in the region of noncollinear ferromagnetic resonance

© A.M. Shutyi, D.I. Sementsov

Ulyanovsk State University,
Ulyanovsk, Russia

E-mail: sementsovdi42@mail.ru

Resonance dynamics of the magnetic moment of a uniaxial ellipsoidal nanoparticle under its magnetic biasing along the symmetry axis and excitation by a transverse high-frequency field is studied with the parameters (frequency, magnetic bias field and shape parameter), corresponding to the noncollinear orientation of equilibrium magnetization and the external static field. We revealed the frequency regions where precession becomes nonlinear at a weak alternating field and dynamic bistability, as well as complex spatial attractors and chaos are implemented.

Keywords: ellipsoidal nanoparticle, ferromagnetic resonance, static and high-frequency field, nonlinearity, effective anisotropy, bistability, regular and chaotic precession.

1. Introduction

It is known that information recording on lattice structures of magnetic nanoparticles (NPs) is based on changing of the equilibrium configuration of magnetic moments of individual NPs due to impact of a pulse of the local magnetic field. Thereat, information can be read by exciting the formed configuration by a weak radio pulse at the frequency of ferromagnetic resonance (FMR) [1–5]. In connection therewith, significant interest is paid to understanding of the fundamental behavior of a spin subsystem in an external static and high-frequency magnetic field in NPs with a complex configuration of internal fields, including exchange, dipole-dipole and magnetostatic fields, a crystalline anisotropy field. Thereat, many FMR features are defined by geometric factors — size of nanoelements, shape and ratio of their sides, spatial arrangement in the structure [6–9]. Therefore, many studies in this field are focused on studies of FMR in thin-film elliptical and rectangular microstrips of a nanometer thickness, which are regarded as one of the main geometric elements for information recording and processing. In the experiment we have observed, along with the main „homogeneous" FMR mode, a thickness-dependent resonance peak, related to heterogeneity of the internal field and, respectively, magnetization distribution on the corners and edges of the microstrips [10,11].

In order to interpret the obtained results, it is also necessary to take into account that the position of the FMR line and its shape substantially depend not only on configuration of the lattice structure, but also on size and symmetry, magnetization equilibrium state, type and value of magnetic anisotropy of individual NPs. Heterogeneity of the internal magnetostatic field near the microstrip boundaries leads to the formation of localized edge modes in the resonance spectrum [12–17].

Special properties of 3D single-domain NPs affecting their dynamic characteristics can also include bistability due to equilibrium orientation states with unequal projections of the magnetic moment, between which controllable transitions with different precession modes during magnetization reversal are possible [18–25]. In order to understand the impact of bistability on FMR, nature of magnetization reversal and dynamics of the magnetic moment in the lattice structure composed of NPs, it is necessary to take into account the above-mentioned factors in a mathematical model describing the high-frequency dynamics in an individual NP.

Equilibrium orientation of magnetization in relation to an external static field can be collinear and noncollinear for a single-domain magnetic uniaxial NP in the shape of an ellipsoid of revolution, when the „easy" axis and magnetic bias field are oriented along the symmetry axis depending on values of system parameters, in particular, on shape parameter n (deviation from spherical shape). Paper [25] studied the peculiarities of resonance dynamics upon activation of a weak transverse high-frequency field for the collinear case. It was shown that dynamic bistability is implemented for the already slightly oblate NP and the FMR deviates from the linear one. In the present paper, a numerical solution of the Landau−Lifshitz−Helmholtz equation (LLH) is used to study the peculiarities of resonance dynamics in the case of noncollinear orientation of magnetization and a static field with a weak transverse high-frequency field. The parameter regions are revealed, which correspond to bistability of precession modes and implementation both of the regular precession modes and high-amplitude chaotic vibrations.

2. Basic relations

Let us consider a sample shaped as an ellipsoid of revolution. We assume that, along with shape anisotropy, the sample has uniaxial anisotropy the easy axis of which coincides with the sample symmetry axis. In this case the free-energy density contains Zeeman energy, anisotropy energy and energy of scattering fields [26,27]:

$$F = -\mathbf{M}(\mathbf{H} + \mathbf{h}) - \frac{K_u}{M^2}(\mathbf{Mn})^2 \frac{1}{2}\mathbf{M}\hat{N}\mathbf{M}. \quad (1)$$

Here $\mathbf{M}$ is NP magnetization, $\mathbf{H}$ and $\mathbf{h}$ are static and high-frequency fields, K_u is the uniaxial anisotropy constant, $\mathbf{n}$ is the unit vector of the anisotropy axis, $\hat{N}$ is the diagonal tensor of demagnetization coefficients whose components correlate as $N_x + N_y + N_z = 4\pi$ and depend on the shape parameter — the ratio of the longitudinal and transverse ellipsoid semi-axes $n = l_p/l_\perp$. The parameters $N_\perp = N_x = N_y$, $N_p = N_z$ and $\Delta N = N_\perp - N_p$ can be conveniently introduced for an ellipsoid of revolution. For oblong and oblate ellipsoids

$$\frac{\Delta N}{2\pi} = 1 - \frac{3}{n^2 - 1}$$
$$\times \left[\frac{n}{\sqrt{n^2-1}}\ln\left(n + \sqrt{n^2-1}\right) - 1\right] > 0, \quad n > 1,$$

$$\frac{\Delta N}{2\pi} = 1 - \frac{3}{n^2 - 1}$$
$$\times \left[\frac{n}{\sqrt{n^2-1}}\arcsin\sqrt{n^2-1} - 1\right] < 0, \quad n < 1. \quad (2)$$

Taking into account the orientation of the „easy" axis of magnetic anisotropy along the sample symmetry axis, the effective anisotropy field $H_{KN} = 2K_u/M_0 + M_0\Delta N$, which determines its resonance behavior (here M_0 is the saturation magnetization), can be conveniently introduced in the consideration. An analysis shows that the effective anisotropy field has regions of both negative and positive values (depending on n). For the used material parameters of the nanoparticle $M_0 = 800\,\text{Gs}$ and $K_u = 10^5\,\text{erg/cm}^3$ (close to the parameters of 80Ni20Fe permalloy), the field is $H_{KN} \approx 0$ at $n = 0.94$, the sign of field H_{KN} changes when n changes near this value.

Time dependence of orientation of the vector of $\mathbf{M}$ and, consequently, the precession dynamics of NP magnetization for different cases of magnetic biasing and high-frequency pumping is determined on the basis of a numerical solution of the LLH equation [26,27]:

$$\frac{\partial \mathbf{M}}{\partial t} = -\gamma\mathbf{M} \times \mathbf{H}^{\text{eff}} + \frac{\alpha}{M}\mathbf{M} \times \frac{\partial \mathbf{M}}{\partial M}, \quad (3)$$

where $\gamma = 1.76 \cdot 10^7\,(\text{Oe} \cdot \text{s})^{1-}$ is the magnetomechanic ratio, α is the dimensionless attenuation constant, the effective magnetic field is

$$\mathbf{H}^{\text{eff}} = -\frac{\partial F}{\partial \mathbf{M}} = \mathbf{H} + \mathbf{h} + \frac{2K}{M_0}\mathbf{n} + \hat{N}\mathbf{M}. \quad (4)$$
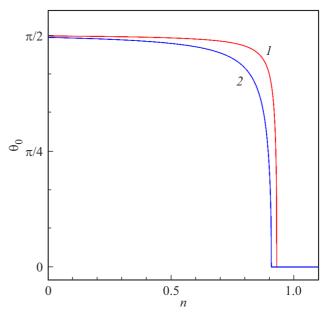
Figure 1. Dependences of the equilibrium polar angle of NP magnetization on shape parameter n at $H = 50,\ 150\,\text{Oe}$ (curves *1, 2*).

The equilibrium values of the polar θ_0 and azimuthal φ_0 angles, which determine the direction of the vector of $\mathbf{M}$ in relation to the ellipsoid symmetry axis (the OZ axis) and the perpendicular axis (for example, OX), are found from the condition $\partial F/\partial\varphi = \partial F/\partial\theta = 0$. There is no dependence on the azimuthal angle during magnetic biasing of an ellipsoidal NP along the symmetry axis ($\mathbf{H} \parallel \mathbf{n} \parallel OZ$) in the basal plane, and equilibrium angle φ_0 can be taken equal to zero. For an oblong and spherical NP (at $n \geq 1$), the equilibrium polar angle is $\theta_0 = 0$ at any value of field H. This value of angle θ_0 also remains for an oblate NP ($n < 1$) up to the value $\Delta N = -(H + H_u)/M_0$. With further decrease in n, the angle θ_0 changes in accordance with the expression

$$\cos\theta_0 = -H(H + \Delta N M_0)^{-1}. \quad (5)$$

Fig. 1 shows the dependence of equilibrium polar angle $\theta_0 = \arccos(M_z/M_0)$ for NP magnetization on shape parameter n, obtained for the two external field values of $H = 50,\ 150\,\text{Oe}$. It can be seen that the vector of $\mathbf{M}$ in the equilibrium state at the given values of the magnetic bias field remains parallel to the external field and the NP symmetry axis only at $n > (0.928,\ 0.906)$ (curves *1, 2* respectively). At smaller values of the shape parameter the angle starts abruptly increasing and reaches a value close to $\pi/2$. The frequency of resonance precession of magnetization in general is determined by expression

$$\omega_r = \frac{\gamma}{M_0\sin\theta_0}\left[\left(\frac{\partial^2 F}{\partial\varphi^2}\right)_0\left(\frac{\partial^2 F}{\partial\theta^2}\right)_0 - \left(\frac{\partial^2 F}{\partial\varphi\partial\theta}\right)_0^2\right]^{1/2},$$
$$(6)$$

where the second derivatives of the free energy are calculated for the equilibrium values of angles φ_0 and θ_0.

During NP magnetic biasing along the easy axis and the symmetry axis $(H \parallel n)$ in the region of values of n where the equilibrium angle θ_0 is zero, the dependence of resonance frequency on external field is determined by the following expression, taking into account (1) and (6)

$$\omega_r = \gamma \left(H + \frac{2K_u}{M_0} + M_0 \Delta N \right). \qquad (7)$$

It should be noted that even rather a small deviation of the NP shape from the spherical shape considerably affects the value of ΔN, which changes the position of the typical values of frequency $\omega_r(0)$ and resonance dependences on the whole. It will be shown below that the shape parameter n also affects the precession dynamics of magnetization of an ellipsoidal NP.

3. Peculiarities of precession dynamics

Let us consider the dynamics of NP magnetization under an alternating magnetic field $\mathbf{h}(t) = \mathbf{h}_0 \sin \omega t$ at $h_0 \ll H$ and orientation $\mathbf{h}_0 \perp \mathbf{H} \parallel OZ$. Then it will be assumed that field $\mathbf{h}(t)$ is polarized along the OY axis. A numerical solution of equations (3) was done by the Runge−Kutta method. Let us consider two cases — collinearity and non-collinearity of the vectors of $\mathbf{M}_0$ and $\mathbf{H}$.

Resonance dynamics of magnetization with a colinear orientation of the vectors of $\mathbf{M}_0$ and $\mathbf{H}$ was considered in [25]; it was shown that high angles of resonant precession are implemented in case of transverse pumping by a weak alternating field (the amplitude at these angles is $0.5M_0$); moreover, there are elliptical perturbations of the
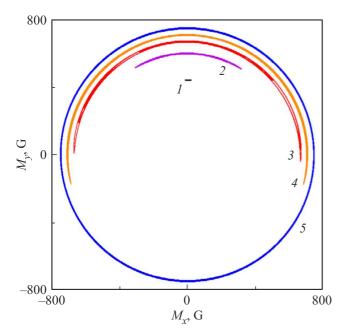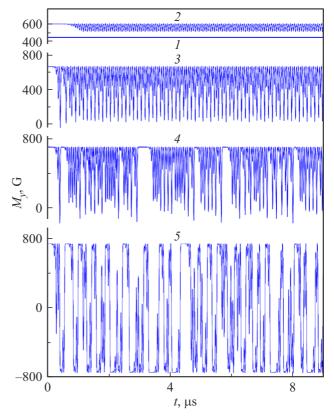

Figure 3. Time dependence of component M_y at $H = 150$ Oe, $h = 0.1$ Oe, $n = 0.9, 0.89, 0.88, 0.87$, (curves *1−5*), $\omega = 1 \cdot 10^8\,\mathrm{s}^{-1}$ (curves *1−3, 5*), $\omega = 1.05 \cdot 10^8\,\mathrm{s}^{-1}$ (curve *4*).

precession trajectory and regions with dynamic bistability are frequently observed.

Let us now consider the magnetization dynamics of a NP where the equilibrium orientation of the vector of $\mathbf{M}$ does not coincide with the OZ symmetry axis, while the equilibrium polar angle is $\theta_0 \neq 0$. This region in Fig. 1 corresponds to a non-linear dependence of angle $\theta_0(n)$.

Fig. 2 shows the projects (onto the XY plane) of NP magnetization at $H = 150$ Oe and values of shape parameter $n = 0.9, 0.89, 0.88, 0.87, 0.85$ (curves *1−5*) during precessional motion under the action of an alternating field, linearly polarized along the Y axis, with $h_0 = 0.1$ Oe and $\omega = 1 \cdot 10^8\,\mathrm{s}^{-1}$ (curves *1−3, 5*), $\omega = 1.05 \cdot 10^8\,\mathrm{s}^{-1}$ (curve *4*). It can be seen that an increase of NP oblateness (i.e. decrease of n) results in an increase of the arc, covered by precession dynamics, which becomes a circle at $n = 0.85$. Threat, precession amplitude considerably depends on alternating field parameters. It should be noted that, along with the given modes, „symmetrical" modes, where the y-component of precessional magnetization is located chiefly in the negative half-plane, are implemented at the same parameters. It indicates the presence of dynamic bistability in precession modes of NP magnetization.

Fig. 3 shows the time dependence of the y-component of magnetization for the cases which satisfy Fig. 2. It is
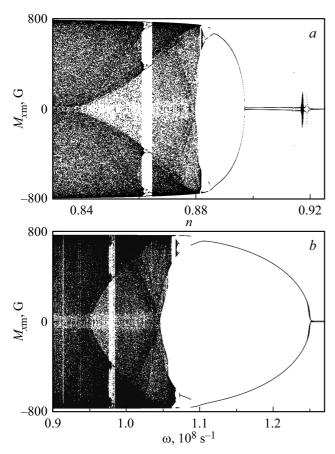

Figure 2. Projection of NP magnetization to XY plane with $n = 0.9, 0.89, 0.88, 0.87, 0.85$ (curves *1−5*) and $\omega = 1 \cdot 10^8\,\mathrm{s}^{-1}$ (curves *1−3, 5*), $\omega = 1.05 \cdot 10^8\,\mathrm{s}^{-1}$ (curve *4*), $H = 150$ Oe, $h_0 = 0.1$ Oe.

near the equilibrium position is still large. Low-amplitude vibrations ($|M_{xm}| \approx 10\,\text{G}$) arise when $0.897 < n < 0.92$. Further decrease of n results in a fast rise of the amplitude of the regular precession dynamics of magnetization to $|M_{xm}| \approx 650\,\text{G}$. Then the vibration trajectory becomes complicated, and at $n < 0.882$ the dynamics enters the region of chaotic vibrations where there are narrow regions of regular precession with complex trajectories and a period which is divisible by the alternating field period. Diagram (*b*) is identical: precession is almost absent at the alternating field frequency $\omega \geq 1.25 \cdot 10^8\,\text{s}^{-1}$ (i.e. the said
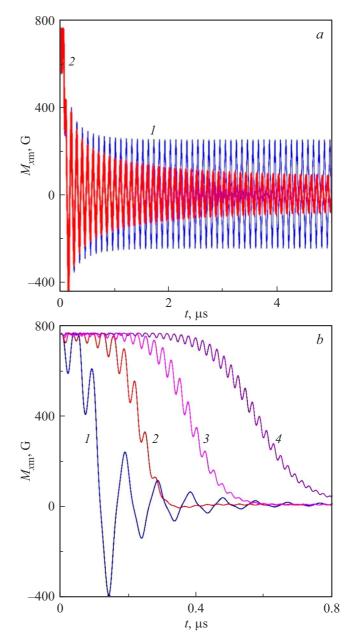

Figure 4. The extreme component M_{xm} vs. parameter n at $\omega = 1 \cdot 10^8\,\text{s}^{-1}$ (*a*) and vs. frequency at $n = 0.87$ (*b*), $h_0 = 0.1\,\text{Oe}$, H=100 Oe.

seen that vibrations with a small precession arc are close to harmonic ones. Irregularity of vibrations increases with a decrease of n and an increase of the precession arc; this irregularity at first affects their amplitude only, but then also the time repeatability of the precession mode. Thereat, the said irregularity becomes most pronounced for the circular projection of the trajectory.

For a more complete analysis of the influence of NP oblateness on magnetization dynamics, we will plot bifurcation diagrams, i.e. dependences of the extreme value of a component of magnetization **M** (here the x-component ($M_{xm} \equiv M_{x\,\text{max}}, M_{x\,\text{min}}$) on shape parameter n at $\omega = 1 \cdot 10^8\,\text{s}^{-1}$ (*a*) and on alternating field frequency at $n = 0.87$ (*b*) with the values $h_0 = 0.01\,\text{Oe}$ and $H = 100\,\text{Oe}$ (Fig. 4). In the absence of magnetization precession, the variable value (n or ω) in the diagram corresponds to one point only; in case of regular vibrations — two or a denumerable number of points; if the parameter value in the diagram corresponds to a non-denumerable number of points (which merge into dark regions with an increase of numerical modeling time), a chaotic dynamic mode arises. Diagram (*a*) shows that precession is almost absent in case of sufficiently small oblateness ($0.92 < n < 1$), since the effective magnetic field which holds magnetization

Figure 5. Time dependence of the component M_x under NP magnetization reversal due to the action of alternating field $h_y(t)$ at frequencies $\omega = (1.24, 1.25) \cdot 10^8\,\text{s}^{-1}$ (*a* — curves *1, 2*) and $\omega = (1.3, 2, 2.5, 3) \cdot 10^8\,\text{s}^{-1}$ (*b* — curves *1−4*), $n = 0.87$, $h_0 = 0.1\,\text{Oe}$, $H = 100\,\text{Oe}$.
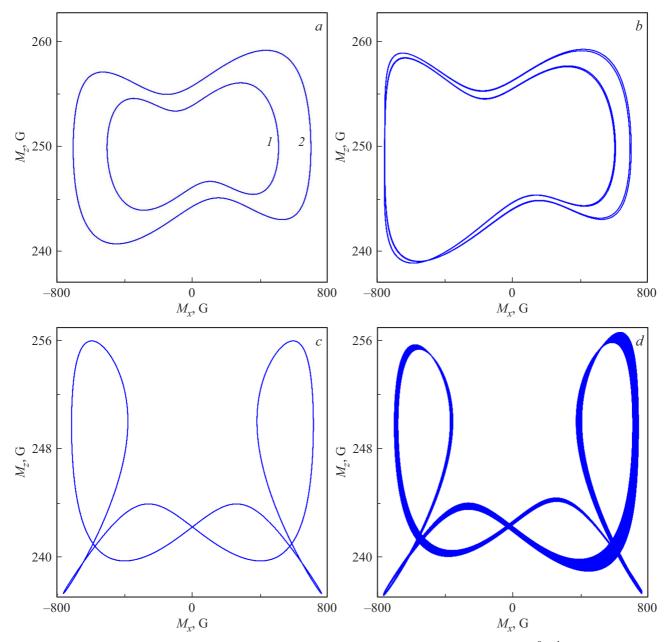
Figure 6. Projections of trajectories of the vector of **M** in case of regular dynamics at $\omega = (1.2, 1.12) \cdot 10^8 \, \text{s}^{-1}$ (a — curves $1, 2$) and $\omega = (1.07, 0.98) \cdot 10^8 \, \text{s}^{-1}$ (b, c); in case of a weak chaotic nature at $\omega = 0.977 \cdot 10^8 \, \text{s}^{-1}$ (d); $h_0 = 0.1 \, \text{Oe}$, $H = 100 \, \text{Oe}$, $n = 0.87$.

parameters are rather far from the resonance values), the amplitude of regular vibrations increases to $|M_{xm}| \approx 750 \, \text{G}$ with a frequency decrease, the dynamics of magnetization at $\omega \leq 1.07 \cdot 10^8 \, \text{s}^{-1}$ is in the chaos region which includes narrow regions of the regular precession. The structure of the given diagrams also shows that the attractors of chaotic modes will change with a change of the given parameters.

To support the aforesaid, Fig. 5, a, b shows the time dependence of component M_x for a NP with shape parameter $n = 0.87$ in static field $H = 100 \, \text{Oe}$ upon activation of alternating field $h_y(t)$, the amplitude of which is $h_0 = 0.1 \, \text{Oe}$, and frequency is $\omega = (1.24, 1.25) \cdot 10^8 \, \text{s}^{-1}$ (a — curves $1, 2$) and $\omega = (1.3, 2, 2.5, 3) \cdot 10^8 \, \text{s}^{-1}$ (b —

curves $1-4$). In the initial state, $M_y(0) = 0$, and the polar angle corresponds to the equilibrium value for the given n and H. It can be seen that all frequencies in the case (b) are in the region which corresponds to the absence of a stationary vibration mode (see the bifurcation diagram). Therefore, upon activation of a high-frequency field, the NP magnetic moment in the mode of quickly decaying vibrations passes into the rest state within a relatively short time interval ($\tau < 1 \, \mu\text{s}$). In the case (a), the frequency for curve 1 is in the region of high-amplitude vibrations, that's why magnetization goes from the initial state under the action of an alternating field to a steady-state vibration mode with an amplitude considerably different from zero.
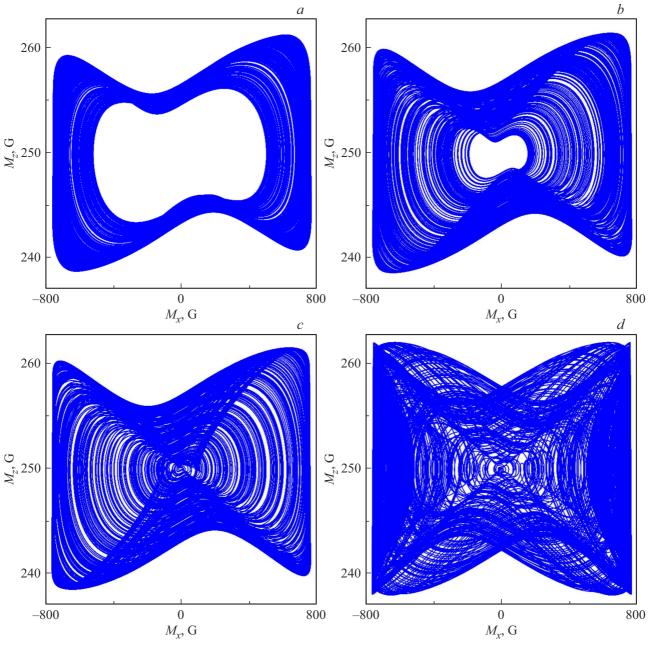
Figure 7. Projections of trajectories of the vector of **M** in case of chaotic dynamics at $\omega = (1.06, 1.05, 1.4, 1) \cdot 10^8\,\text{s}^{-1}$ $(a{-}d)$; $h_0 = 0.1\,\text{Oe}$, $H = 100\,\text{Oe}$, $n = 0.87$.

Stationary precession is already absent for curve *2*, while the frequency is near the boundary which separates the region of stationary vibrations and the region without self-sustaining precession modes. Therefore, vibrations generated by the alternating field are transient dynamic states with a long decay time ($\tau \gg 1\,\mu\text{s}$).

As mentioned above, precession modes with arc-shaped projections of trajectories onto the XY plane (see Fig. 2) are related to precession dynamic bistability. To clearly demonstrate the said bistability, let us consider the main regular and chaotic precession modes for a NP with parameter $n = 0.87$, which establish in case of $h_0 = 0.1\,\text{Oe}$

and $H = 100\,\text{Oe}$ at different frequencies. Fig. 6 shows the projections of the trajectories of the vector of **M** onto the XZ plane in case of regular dynamics at frequencies $\omega = (1.2, 1.12) \cdot 10^8\,\text{s}^{-1}$ (a — curves *1, 2*), $\omega = (1.07, 0.98) \cdot 10^8\,\text{s}^{-1}$ (b, c) and in case of a mode with a weak chaotic nature at frequency $\omega = 0.977 \cdot 10^8\,\text{s}^{-1}$ (d). It should be noted that an attractor (d) arises due to chaotization and expansion of the attractor of the regular mode (c). This mode is located in a narrow region of regular dynamics inside the chaos region (see the bifurcation diagram), and chaotic nature of vibrations increases abruptly with a further frequency decrease, and a stochastic mode

with a symmetrical attractor (as distinct from case (d)) arises. The modes (a) have the simplest attractors and establish at relatively high frequencies, up to frequencies at which precession stops. Regular precession (b) has a divisible period in relation to the alternating field period $T = 8\pi/\omega$. The projections of the attractors onto the XZ is a circle in cases (c, d) and an arc in cases (a, b).

Fig. 7 shows the projections of NP magnetization trajectories onto the XZ plane for the above-mentioned parameters of the field and NP oblateness and frequency $\omega = (1.06, 1.5, 1.04, 1) \cdot 10^8\,\mathrm{s}^{-1}$ $(a-d)$; these projections show the development of chaotic nature of dynamics at a slight decrease of alternating field frequency. The maximum chaotic nature arises when the projection of the attractors onto the XY plane becomes a circle (d), these projections are arcs in cases $(a-C)$.

4. Conclusion

The performed analysis shows that FMR of a single-domain NP in the shape of an oblate ellipsoid of revolution and an „easy" axis, coinciding with the symmetry axis, under magnetic biasing along this axis and transverse pumping with a weak alternating field ($h_0 \ll H$) considerably differs in the case of noncollinear orientation of magnetization and static field. The precession modes in case of the previously studied collinear initial orientation are mostly close to a linear magnetic resonance, except the implementation (with weak alternating fields) of high precession angles and nutation motion of magnetization. A noncollinear case occurs in case of a negative difference of the magnetic bias field and the effective anisotropy field. Thereat, the initial orientation of magnetization does not coincide with the anisotropy axis and the magnetic bias field; the direction cone, which is determined by the equilibrium polar angle only, becomes easy. In this case we have bistability of precession modes and, depending on frequency, a weak alternating field excites both regular precession modes, including precession with an amplitude close to M_0, and various high-amplitude chaotic vibrations.

It should be noted that, with the amplitude and frequency of the pumping field used herein, the homogeneous mode is largely removed in terms of frequency from the spin-wave mode, that's why there is no energy transfer from the homogeneous precession to the spin waves and no development of spin-wave instabilities [28].

In conclusion, we also state the limitations imposed on the NP size, which are related to the requirement of magnetization homogeneity [29]: in the presence of a high-frequency field the maximum NP size d must be much smaller than the skin-layer depth δ. For a permalloy NP the condition $d \ll \delta \approx 10^{-4}$ cm must be met; thermal fluctuations may considerably affect the precession dynamics of NP magnetization. Their influence is described by multiplier $(-\Delta U/k_{\mathrm{B}}T)$ [3], where ΔU is the potential barrier separating the „easy" and „hard" directions. Thermal

excitation does not disturb the precession dynamics if the NP size is $d > d_{\min} \approx 10$ nm; the requirement for a single-domain NP, according to which its radius must be less than $R_{cr} \approx \sigma_s/M_0^2$, where surface energy of the domain boundary (for permalloy, $\sigma_s \approx 1\,\mathrm{erg/cm}^2$). Therefore, the requirement for the NP under study is $d < 2R_{cr} \approx 30$ nm.

Thus, the most optimal NP size for FMR observation is $d \in (10 \div 30)$ nm. It should be noted that, according to [30], metal particles with $d \approx 40 \div 50$ nm should be considered single-domain.

Conflict of interest

The authors declare that they have no conflict of interest.

References

[1] E.Z. Meilikhov, R.M. Farzetdinova. J. Magn. Magn. Mater. **268**, 237 (2004).

[2] N. Eibagi, J.J. Kan, F.E. Spada, E.E. Fullerton. IEEE Magn. Lett. **3**, 4500204 (2012).

[3] E.Z. Meilikhov, R.M. Farzetdinova. FTT **56**, *4*, 2326 (2014).

[4] R. Berger, J.-C. Bissey, J. Kliava, H. Daubric, C. Estournéset. J. Magn. Magn. Mater. **234**, 535 (2001).

[5] R.B. Morgunov, A.I. Dmitriyev, G.I. Dzhardimaliyeva, A.D. Pomogaylo, A.S. Rosenberg, Y. Tanimoto, M. Leonowicz, E. Sowka. FTT **49**, *8*, 1436 (2007).

[6] G. Gubbiotti, G. Carlotty, T. Okuno, L. Giovannini, F. Montoncello, F. Nizzoli. Phys. Rev. B **72**, 184419 (2005).

[7] K.D. Usadel. Phys. Rev. B **73**, 212905 (2006).

[8] V.V. Kruglyak, S.O. Demokritov, D. Grundler. J. Phys. D **43**, 264001 (2010).

[9] A. Moser, K. Takano, D.T. Margulies, M. Albrecht, Y. Sonobe, Y. Ikeda, S.H. Sun, E.E. Fullerton. J. Phys. D **35**, *19*, R157 (2002).

[10] V. Flovik, F. Macia, J. M. Hernandez, R. Bručas, M. Hanson, E. Wahlström. Phys. Rev. B **92**, 104406 (2015).

[11] A.M. Biller, O.V. Stolbov, Yu.L. Raikher. Vychislitelnaya mekhanika sploshnykh sred **8**, *3*, 273 (2015) (in Russian).

[12] M.P. Wismayer, B.W. Southern, X.L. Fan, Y. S. Gui, C.-M. Hu, R. E. Camley. Phys. Rev. B **85**, 064411 (2012).

[13] M. Pardavi-Horvath, B.J. Ng, F.I. Gastano, H.S. Körner, C. Garcia, C.A. Ross. J. Appl. Phys. **110**, 053921 (2011).

[14] N. Yu Grigoryeva, D.A. Popov, B.A. Kalinikos. Phys. Solid State **56**, *9*, 1806. (2014).

[15] A.M. Shutyi, D.I. Sementsov. Pisma v ZhETF **99**, *12*, 806 (2014) (in Russian).

[16] C. Wen-Bing, H. Man-Gui, Z. Hao, O. Yu, D. Long-Jiang. Chin. Phys. B **19**, *8*, 087502 (2010).

[17] E.V. Skorohodov, R.V. Gorev, R.R. Ykubov E.S. Demidov, Yu.V. Khivintsev, Y. Filimonov, V.L. Mironov. J. Magn. Magn. Mater. **424**, 118 (2017).

[18] D.V. Vagin, O.P. Polyakov. J. Magn. Magn. Mater. **320**, 3394 (2008)

[19] D. Laroze, P. Vargas, C. Cortes, G. Gutierrez. J. Magn. Magn. Mater. **320**, 1440 (2008).

[20] R.K. Smith, M. Grabowski, R. Camley. J. Magn. Magn. Mater. **322**, 2127 (2010).

[21] M. Phelps, K. Livesey, A. Ferona, R. Camley. Europhys. Lett. **109**, 37007 (2015).

[22] A.M. Shutyĭ, S.V. Eliseeva, D.I. Sementsov. Phys. Rev. B **91**, *2*, 024421 (2015).

[23] A.M. Shutyĭ, D.I. Sementsov. J. Magn. Magn. Mater. **401**, *3*, 1033 (2016).

[24] T.M. Vasilevskaya, A.M. Shutyi, D.I. Sementsov. FTT **64**, *2*, 200 (2022).

[25] A.M. Shutyi, T.M. Vasilevskaya, D.I. Sementsov. FTT **64**, *6*, 646 (2022).

[26] A.G. Gurevich, G.A. Melkov. Magnitnye kolebaniya i volny. Nauka, M. (1994) (in Russian).

[27] V.G. Shavrov, V.I. Shcheglov. Dinamika namagnichennosti v usloviyakh izmeneniya ee orientatsii. Fizmatlit, M. (2019) (in Russian).

[28] P.E. Zilberman, A.G. Temiryazev, M.P. Tikhomirova. ZhETF **108**, 281 (1995) (in Russian).

[29] L.D. Landau, E.M. Lifshitz. Teoreticheskaya fizika. Vol. VIII. Nauka, M. (1982) (in Russian).

[30] S.A. Nepiyko. Fizicheskiye svoistva malykh metallicheskikh chastits. Nauk. dumka, Kiev (1985) (in Russian).